Chemical Physics Letters 470 (2009) 249–254

Contents lists available at ScienceDirect

Chemical Physics Letters

journal homepage: www.elsevier.com/locate/cplett

J coupling and chemical shifts in carbon nanostructures for quantum computing

Alejandro León [a,*], Zdenka Barticevic [b], Mónica Pacheco [b]

[a] Facultad de Ingeniería, Universidad Diego Portales, Ejército 441, Santiago, Chile
[b] Departamento de Física, Universidad Técnica F, Santa María, Casilla 110 V, Valparaíso, Chile

ARTICLE INFO

Article history:
Received 6 November 2008
In final form 13 January 2009
Available online 25 January 2009

ABSTRACT

In this work we have performed calculations for the *J* coupling and chemical shifts of carbon-based nanostructures for NMR quantum computing. The systems postulated are finite carbon nanotubes and finite graphene nanoribbons enriched with ^{13}C atoms and finished on the edges with hydrogen atoms. The nuclear spins of ^{13}C and hydrogen are considered as qubits, in order to make calculations of quantum computing. We have determined the electronic properties of our proposed systems using first-principles calculations. From these results we have identified the most relevant NMR parameters that characterize the different systems, by using the theory of double perturbation to first order in the energy of the molecules studied.

1. Introduction

The physical implementation of quantum computing is a very attractive topic to research due to the possibility of solving multiple computing problems which cannot be solved with classical digital computers [1]. Since the use of the nuclear spin in quantum computing was proposed [2], it led to the problem of how to use an array of nuclei at room temperature, and also how to determine the type of algorithms to be used in order to obtain outlet readings with this array. This problem was solved by preparing the system in effectively pure states [3] and adding classical steps to process the information [4]. Several experimental works have reported significant advancements using these techniques in the development of quantum computing [5,6]. Besides, some NMR studies on molecules in liquid phases and the use of well-known quantum algorithms on a small number of qubits have been published by different research teams [7–10]. There are studies reporting quantum information processes using NMR on solid state samples [11], and also studies of quantum computing with carbon nanostructures [12].

After the discovery of the molecule of fullerene [13], new carbon-based structures have been synthesized and characterized. The magnetic, transport and optical properties of these nanostructures have been intensively studied [14,15]. In particular, the development of the techniques of synthesis and characterization of nanotubes has allowed the study of their physical properties and their dependence with its structural parameters [16,17]. Recently, several groups have reported measurement of NMR in carbon nanotubes [18].

This Letter presents a study on *J* couplings and chemical shifts for quantum computing on finite CNTs and finite graphene nanoribbons, enriched with atoms of ^{13}C and passivated with hydrogen atoms. The qubits correspond to the nuclear spins of these atoms. In contrast with NMR experiments with other molecules, in these systems the concentration of isotopes and the number of qubits on a region of the nanotube or nanoribbon can be manipulated.

2. Mathematical model of nuclear spins

When quantum computing is performed with NMR, we are working with an array of systems which initial state can be represented by the density matrix:

$$\rho = \frac{e^{-\beta H}}{Z}, \tag{1}$$

where $Z = tr(e^{-\beta H})$ is the partition function, with $\beta = 1/k_B T$. At room temperature we can use the approximation valid for n spins:

$$\rho \approx 2^{-n}[1 - \beta H]. \tag{2}$$

The Hamiltonian representing n nuclear spins, usually of different atoms, can be written:

$$H = H^{cs} + H^{J} + H^{rf} + H^{D} + H^{env}. \tag{3}$$

The first term represents the interaction of spins with the static magnetic field, incorporating the chemical shift. This term has the following form:

$$H^{cs} = -\boldsymbol{\mu}^T \mathbf{B}^{ext} \tag{4}$$

with

$$\boldsymbol{\mu}^T = \sum_i \boldsymbol{\mu}_i (1 - \boldsymbol{\sigma}_i),$$

* Corresponding author.
E-mail address: alejandro.leon@udp.cl (A. León).

0009-2614/$ - see front matter © 2009 Elsevier B.V. All rights reserved.
doi:10.1016/j.cplett.2009.01.052

where $\boldsymbol{\sigma}_i$ is the 'nuclear shielding tensor', and the nuclear magnetic dipole moments are given by $\boldsymbol{\mu}_i = \gamma_i \hbar \mathbf{I}_i$, with γ_i are the giromagnetic ratios and $\mathbf{I}_i$ the nuclear spin angular momentum operators.

For a liquid sample, the main axis of the ellipsoid which represents the anisotropy of the chemical shift can be aligned with the rotation axis. With this procedure, the anisotropy can be reduced and we can write the term H^{cs} as a function of the values of the isotropic Larmor frequencies ω_i:

$$H^{cs} = \sum_i \frac{\mu_i(1-\sigma_i)}{2} = \sum_i \frac{\hbar\omega_i}{2}\mathbf{Z}_i, \tag{5}$$

where $\mathbf{Z}_i$ is the Pauli matrix for the nuclei *i*.

The H^J term represents the indirect interaction between spins:

$$H^J = \sum_{i,j} \boldsymbol{\mu}_i \mathbf{K}_{ij} \boldsymbol{\mu}_j, \tag{6}$$

where $\mathbf{K}_{ij}$ is the 'indirect reduced coupling tensor' for nucleus *i* and *j*. The relationship between this tensor and the physical quantity $\mathbf{J}_{ij}$ which is measured in the experiments is: $\mathbf{J}_{ij} = \frac{\hbar}{2\pi}\gamma_i\gamma_j\mathbf{K}_{ij}$.

The spin direct dipolar interaction can be written:

$$H^D = \sum_{i,j} \frac{\gamma_i\gamma_j\hbar}{4r^3}\left[\mathbf{I}_i\cdot\mathbf{I}_j - 3(\mathbf{I}_i\cdot\hat{\mathbf{n}})(\mathbf{I}_j\cdot\hat{\mathbf{n}})\right]. \tag{7}$$

Here *r* is the internuclear distance, the $\hat{n}$ vector points in the direction of the line joining the nuclei. If the sample is considered liquid, this dipolar interaction is negligible.

The radio-frequency term can be written as follow:

$$H^{rf} = \sum_i C\left[\mathbf{X}_i\cos(\omega_{rf}t) + \mathbf{Y}_i\sin(\omega_{rf}t)\right], \tag{8}$$

where the constant *C* depends on the magnitude of the amplitude of the radio-frequency electromagnetic field which rotates at ω_{rf}, and $\mathbf{X}_i, \mathbf{Y}_i$ are the Pauli matrices.

Finally, the last term of Eq. (3) represents the interaction of the spins with the environment. Different experimental techniques have been used to measure the decoherence times. In our study we consider operations before losing the coherence, for this reason, from now ahead we will neglect the term H^{env}. Therefore, the Hamiltonian can be written as follows:

$$H = \sum_i \frac{\hbar\omega_i}{2}\mathbf{Z}_i + \sum_{ij}\frac{2\pi}{h}(\gamma_i\gamma_j)^{-1}\boldsymbol{\mu}_i\mathbf{J}_{ij}\boldsymbol{\mu}_j + \sum_i C\left[\mathbf{X}_i\cos(\omega_{rf}t) + \mathbf{Y}_i\sin(\omega_{rf}t)\right]. \tag{9}$$

3. Systems characterization and quantum computation

3.1. Graphene nanodots

In this section we study graphene nanodots (GNDs) which are graphene nanoribbons of finite size. In fact, these small ribbons correspond to aromatic molecules such as $C_{20}H_{12}, C_{28}H_{14}, C_{36}H_{16}$, $C_{44}H_{18}, C_{30}H_{16}$, and $C_{40}H_{20}$, which we will denote like *Dot*(*nm*), where *n* represents the number of carbon atoms passivated with hydrogen atoms along one of the armchair edges of the ribbon and *m*, the number of carbon atoms passivated with hydrogen atoms along one of the zig-zag edges of the ribbon [19]. These GNDs are shown at the right side of Fig. 1.

To determine the parameters NMR, we first optimize the geometry of the system postulated by means of the method 'quasi Newton approach' [20] then, we calculate the total energy of the system using first-principles calculations based on the density functional GGA Becke–Perdew [21,22]. We use Slater type orbitals and double zeta polarized basis (DZP), by using the ADF software [23]. Finally,

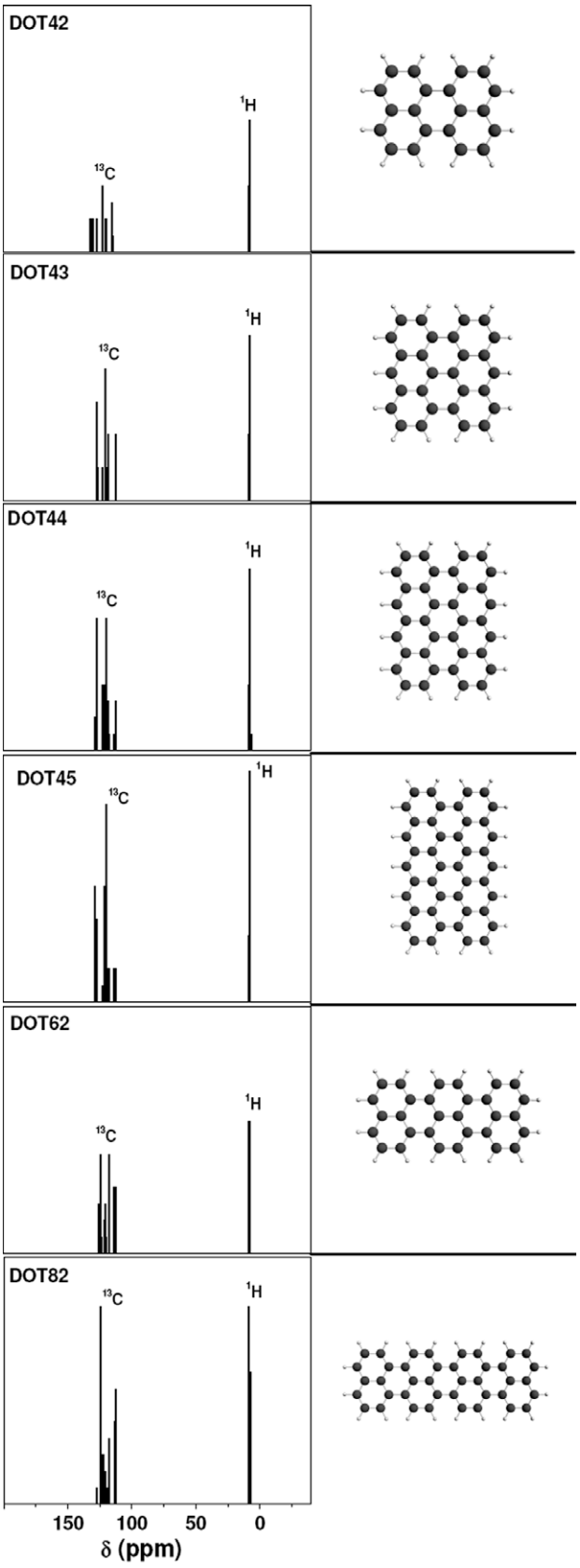

Fig. 1. Chemical shifts relative to the value for tetramethylsilane (TMS) computed at the same level of theory for each GND showed at the right hand side of the figure.

the shielding and indirect coupling tensors for the molecule are obtained as double first-order perturbations of the total energy $E = \langle \Psi | H | \Psi \rangle$ of the molecule [24].

Fig. 1 shows the results reported as chemical shifts relative to the value for tetramethylsilane (TMS) computed at the same level of theory.

In these nanodots it is possible to distinguish three types of topologically inequivalent hydrogen atoms. One hydrogen bonded to a carbon atom settle along an armchair edge, one hydrogen bonded to a carbon along a zig-zag edge and one hydrogen bonded to a carbon at the corner of the ribbon. Respecting to the values of the chemical shift, our results show that the corner hydrogen atoms are equivalent to those of the zig-zag edge. This behaviour is the same for all the six studied GNDs. In the case of the carbon atoms of the edges, the chemical shifts are different for the three inequivalent atoms. The calculated mean values of the coupling constant J between an hydrogen atom and the three type of nearest carbon atoms are displayed in Table 1, for the six nanostructures considered. There J_A means coupling along the armchair edge, J_Z along the zig-zag edge, and J_C corresponds to coupling at the corner.

We can appreciate that, except for the smallest structure DOT42, for all GNDs having more zig-zag edges than armchair edges, the J couplings between the hydrogen and carbon atoms are all different. Otherwise, in GNDs with mostly armchair edges, the J couplings with corner atoms or with zig-zag atoms is almost the same.

Our results also indicate that the edge carbon atoms are coupled to their nearest neighbors internal carbon atoms. In the quantum computation processes, for what we are postulating these structures, we will disconnect the internal atoms and we will only work with the hydrogen atoms and with the carbon atoms of the edges. To achieve the disconnection we must identify the chemical shifts of the internal carbon atoms and the value of the J couplings between them and those in the edges. We found that the chemical shifts of the carbon atoms of the six structures considered present similar patterns. The GNDs with mostly zig-zag edges present sharper resonances for signal control effects of the carbon atoms.

As an example of the followed procedure to obtain the Hamiltonian of the system, we will consider the case of the DOT45 shown in Fig. 2. There we have labeled the three types of inequivalent carbon atoms and their firsts nearest neighbors. A: armchair, Z: zig-zag, C: corner, X: first neighbor armchair, Y: first neighbor zig-zag. In Fig. 3 it is shown the ^{1}H NMR spectrum and in Fig. 4 the corresponding ^{13}C NMR spectrum for the molecule DOT45, for a magnetic field of the 18.6 (T).

We found the following values for the J coupling between the edge carbon atoms and their first neighbors: $J_{Z-Y} = 46.4$ Hz, $J_{A-X} = 50.0$ Hz, $J_{Z-C} = 45.4$ Hz, $J_{A-C} = 42.0$ Hz. With the knowledge of the resonance positions of the neighboring edge atoms and the J coupling constants, it is possible to remove the effect of these couplings by means of refocusing techniques. By other hand, the atoms located far away from the edges are uncoupled of the edge atoms, and their chemical shifts correspond to different frequency values. Therefore, we can implement a system of five qubits (two inequivalent hydrogens and three inequivalent carbon edge atoms) with three different J couplings given by: J_A, J_Z and J_C). The Hamiltonian of this system can be written as:

$$H = \frac{\hbar}{2}\sum_{j=1}^{5}\omega_j \mathbf{Z}_j + \frac{\pi\hbar}{2}\sum_{i<k} J_{ik}\mathbf{Z}_i\mathbf{Z}_k. \quad (10)$$

Once the Hamiltonian has been obtained we can applied standard pulses control techniques to our system for obtaining the universal

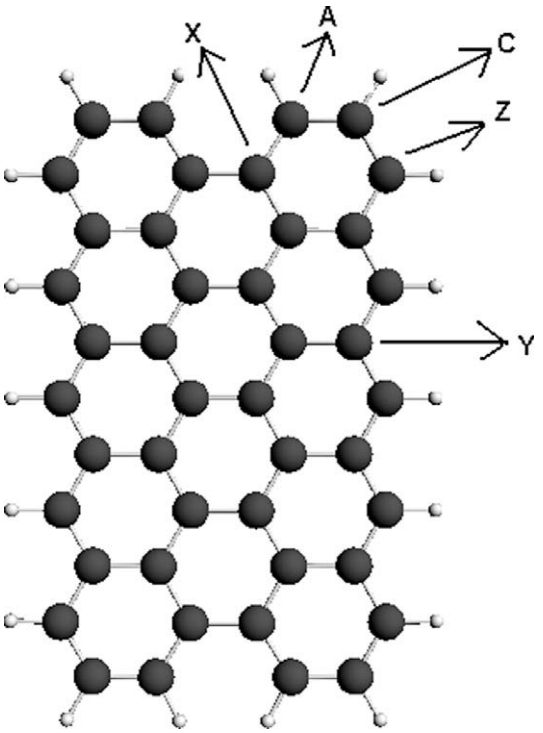

Fig. 2. The three types of non-equivalent edge carbon atoms and their first nearest neighbors. A: armchair, Z: zig-zag, C: corner, X: armchair first neighbor, and Y: zig-zag first neighbor.

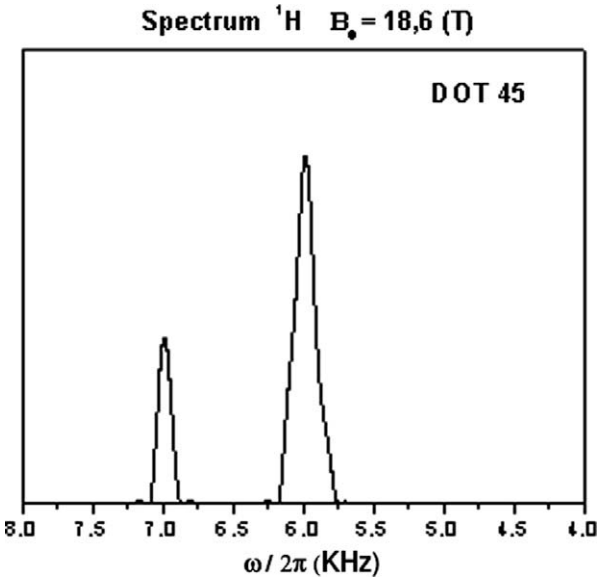

Fig. 3. NMR spectrum of the hydrogen in the molecule DOT45.

Table 1
J couplings between H and the inequivalent edge ^{13}C in GNDs.

	J_A (Hz)	J_Z (Hz)	J_C (Hz)
Dot42	157.2	163.3	163.2
Dot43	154.1	158.0	160.6
Dot44	154.7	157.3	160.8
Dot45	154.6	158.2	160.7
Dot62	153.9	160.3	160.5
Dot82	153.8	160.3	160.5

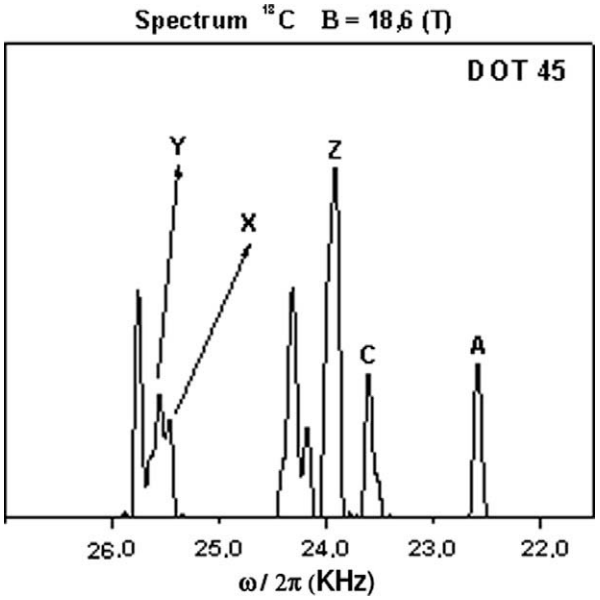

Fig. 4. ^{13}C NMR spectrum of the carbon in the molecule DOT45.

unitary operations. The number of qubits can be modified by means of refocusing operations [25].

3.2. Finite carbon nanotubes

The second system under study is a set of finite armchair and zig-zag carbon nanotubes, enriched with ^{13}C atoms and passivated with hydrogen atoms. The methodology to determine the NMR parameters is the same that we adopted in the last section, for the GNDs. In Fig. 5 we show the chemical shifts for six of these nanotubes, calculated relative to the TMS molecule. The labeling adopted in this case is NTnml, where (n,m) correspond to the indexes of the CNT and the last number l, is proportional to the tube length.

Our calculations show that in the case of finite nanotubes only one signal is registered corresponding to the hydrogen atoms, but multiples signals are registered from the carbon atoms. A remarkable result is the clear signal for the carbon atoms obtained for CNTs as compared with the GNDs. Therefore we may infer that the control for the quantum information processes would be much more efficient in CNTs. We can have systems formed by 3, 4 or 5 qubits depending of the number of carbon atoms considered.

We show in Fig. 6 the detailed spectra for the three (3,3) armchair CNTs, NT333, NT334 and NT335, for a magnetic field corresponding to 9.32 (T). We can observe that the number of peaks in the spectrum coincides with the inequivalent carbon atoms along the nanotube sections. Moreover, the position of the peak corresponding to an edge atom (E), changes with the tube length. The same occurs with the first (V1) or second (V2) neighboring atoms. A similar behaviour is displayed by the wider armchair (4,4) and zig-zag (3,0) CNTs. The corresponding ^{13}C spectra for these systems are showed in Figs. 7 and 8, respectively.

Although the studied systems are small molecules we can get important conclusions valid for single-walled CNts of greater diameters. In Table 2 we show the calculated J coupling between the hydrogens and the edge carbon atoms. We also found that the coupling between the carbon atoms of the edges is in the order of 50 Hz for narrow armchair CNTs, and 47 Hz for wider armchair CNTs. Besides, the couplings between carbon edge atoms and its internal first neighboring atoms are in the order of 40 Hz, while the corresponding coupling with its second neighboring atoms is in the order of 1 Hz.

In Table 3 it is shown the position of the chemical shifts of the hydrogen atoms in the six CNTs for 100 MHz. From these results we deduce that we can have systems composed by three qubits

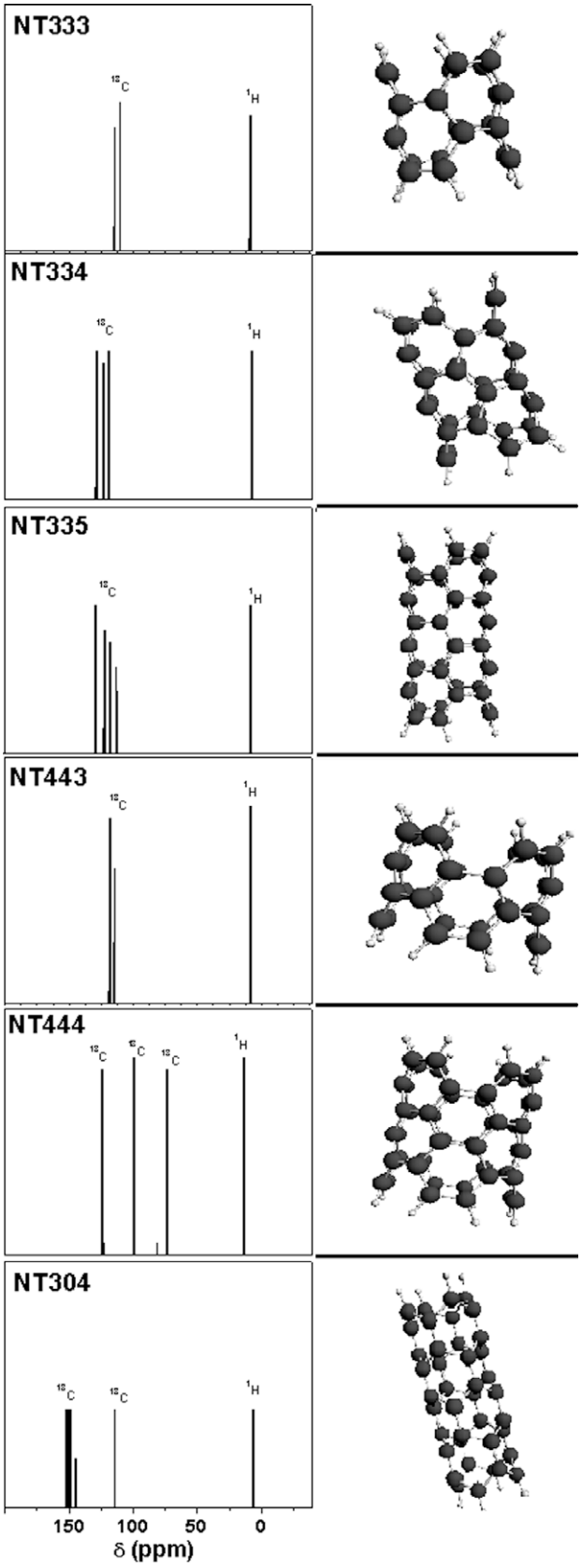

Fig. 5. Chemical shifts relative to the value of tetramethylsilane (TMS) and scheme of finite nanotubes.

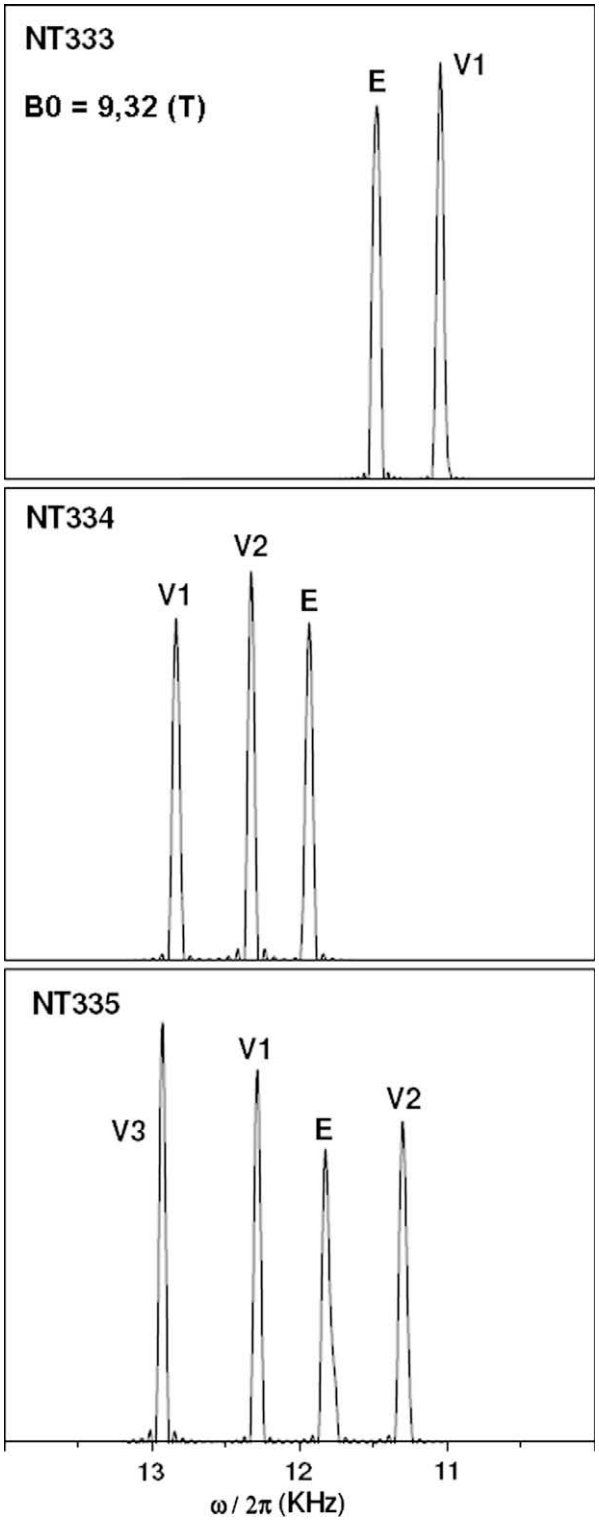

Fig. 6. NMR spectra of the inequivalent carbon atoms in the nanotubes NT333, NT334 and NT335, registered at 9,32 (T).

for NT333 (hydrogen, edge carbon and internal carbon), and systems composed by 4, 5, or 6 qubits for others CNts, if we consider the more internal atoms. Similarly to the case of the GNDs, we can applied refocusing techniques to disconnect spines and for changing the number of qubits of the system. With the knowledge of the NMR spectra and the coupling constants, it is possible to develop universal quantum control operations.

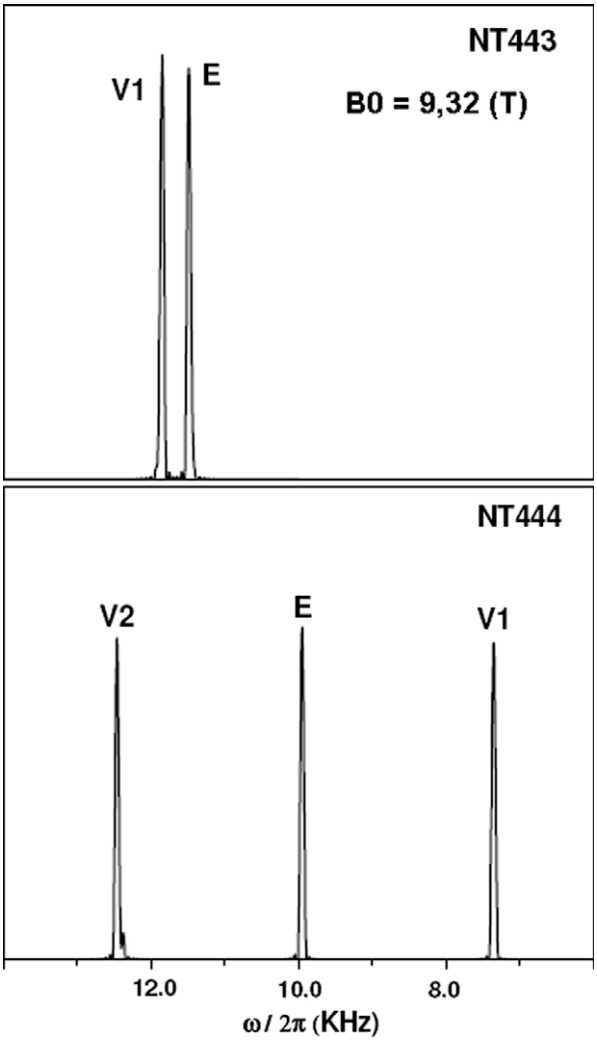

Fig. 7. NMR spectra of the inequivalent carbon atoms in the nanotubes NT443 and NT444 for a magnetic field of the 9,32 (T).

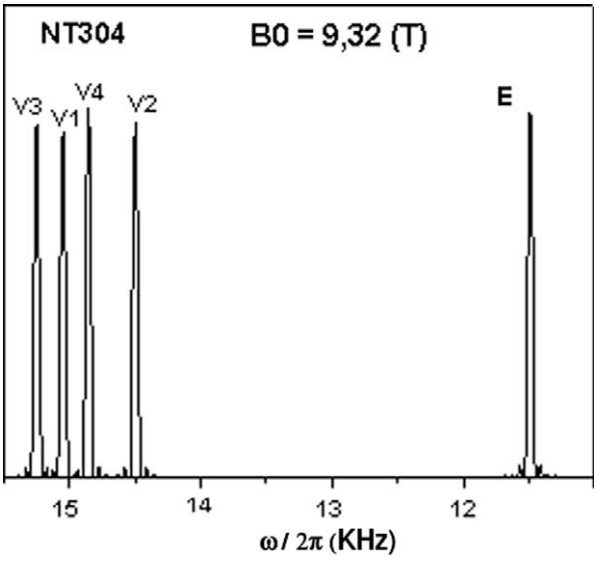

Fig. 8. NMR spectrum of the inequivalent carbon atoms in the nanotubes NT304 registered at 9,32 (T).

Table 2
J couplings between H and edge ^{13}C in finite carbon nanotubes.

Nanotube	J_{CH} (Hz)
NT333	166.3
NT334	169.4
NT335	168.5
NT443	161.2
NT444	160.3
NT304	169.6

Table 3
Chemical shifts of finite carbon nanotubes.

Nanotube	Chemical shifts (Hz)
NT333	873
NT334	763
NT335	882
NT443	851
NT444	1318
NT304	666

4. Summary and conclusions

In relation to the results obtained for the different system studied we can say that the graphene nanodots present a great advantage from the point of view of the flexibility in achieving a variety of different geometrical designs by means of lithographical techniques [26]. However, in these systems the spectra for the carbon atoms show relatively wide signals and it implies that the control methodology must be optimized in order to obtain reliable results. We believe that the continue advance in the experimental protocols for the synthesis of these molecules will allow to control the ^{13}C doping for a given desired architecture for quantum computing. By other hand, the finite CNTs presents very pure signals of the hydrogen and carbon atoms, with a very good spectral resolution. This allows to expect high fidelity quantum control operations. The main disadvantage of the CNTs is the actual experimental difficulty to synthesize samples with similar sizes and diameters.

An important to mention that the decision of placing hydrogen atoms at the edges of the carbon nanostructures has to be with the possibility of identifying the inequivalent carbon atoms in the CNT. We could passivate the ends of the tubes with other kind of atoms, active or not for NMR, but this study will remain valid in relation to the signals of the internal atoms. In addition we like to point out that our results for the chemical shifts of (4,4) CNts show good agreements with the theoretical results for CNTs reported by Besley et al. [27]. The comparison is only valid for the central atoms.

The most important contribution of this report is the calculation of the indirect coupling constants between the nuclei for the studied nanostructures. The knowledge of these parameters allows to implement the sequence of intervals of free evolution between control pulses applied to the system.

This study leads to the conclusion that it is possible to develop quantum operations using NMR in a carbon nanocluster. In these systems it is possible to have a variable number of atoms with nuclear spins and consequently a variable number of qubits in the array. We now that the total signal decreases exponentially as the number of qubits considered into an effective pure state using labeling techniques, for constant initial state temperature. Methods for circumventing the limitations of labeling techniques exist. One possibility is to polarize the nuclei through some physical mechanism. Another possibility is the use of a different labeling scheme. An improved version of this method has been developed which achieves the entropic limit. This scheme does not have any exponential cost; the compression can be achieved using only a polynomial number of basic operations [28].

Acknowledgements

We thank financial support from CONICYT/Programa Bicentenario de Ciencia y Tecnología (CENAVA, Grant ACT27), Universidad Diego Portales for 'Proyecto Semilla 2007–2008-primavera', and UTFSM for internal grants.

References

[1] M.A. Nielsen, I.L. Chaung, Quantum Computation and Quantum Information, Cambridge University Press, Cambridge, 2003.
[2] D.P. DiVincenzo, Phys. Rev. A 51 (1995) 1015.
[3] D.G. Cory, A.F. Fahmy, T.F. Proc, Nat. Acad. Sci. USA 94 (1997) 1634.
[4] N. Gershenfeld, I.L. Chuang, Science 275 (1997) 350.
[5] E. Knill, I. Chuang, R. Laflame, Phys. Rev. A 57 (1998) 3348.
[6] L.M.K. Vandersypen, C.S. Yannoni, M.H. Sherwood, I.L. Chuang, Phys. Rev. Lett. 83 (1999) 3085.
[7] I.L. Chuang, L.M.K. Vandersypen, X.L. Zhou, D.W. Leung, S. Lloyd, Nature 393 (1998) 143.
[8] D.G. Cory et al., Phys. Rev. Lett. 81 (1998) 2152.
[9] M.A. Nielsen, E. Knill, R. Laflamme, Nature 396 (1998) 52.
[10] J.A. Jones, M. Mosca, R.H. Hansen, Nature 393 (1998) 344.
[11] G.M. Leskowitz, N. Ghaderi, R.A. Olsen, L.J. Mueller, J. Chem. Phys. 119 (2003) 1643.
[12] J.J.L. Morton, A.M. Tyryshkin, A. Ardavan, S.C. Benjamin, K. Porfyrakis, S.A. Lyon, G.A.D. Briggs, Nature Phys. 2 (2006) 40.
[13] H.W. Kroto, J.R. Heath, S.C. O'Brien, R.F. Curl, R.E. Smalley, Nature 318 (1985) 162.
[14] E. Lo, B.R. Judd, Phys. Rev. Lett. 82 (1999) 3224.
[15] A.V. Kikolaev, K.H. Michel, J. Chem. Phys. 117 (2002) 4761.
[16] A.G. Marinopoulos, L. Wirtz, A. Marini, V. Olevano, A. Rubio, L. Reining, Appl. Phys. A 78 (2004) 1157.
[17] M. Dresselhaus, G. Dresselhaus, R. Saito, A. Jorio, Phys. Rep. 409 (2005) 47.
[18] A. Kitaygorodskiy et al., J. Am. Chem. Soc. 127 (2005) 7517.
[19] O. Hod, V. Barone, G.E. Scuseria, Phys. Rev. B 77 (2008) 035411.
[20] L. Versluis, The Determination of Molecular Structures by the HFS Method, University of Calgary, 1989.
[21] A.D. Becke, Phys. Rev. A 38 (1988) 3098.
[22] J.P. Perdew, Phys. Rev. B 33 (1986) 8822.
[23] http://www.scm.com/.
[24] J. Autschbach, Struct. Bonding (2004) 112.
[25] L.M.K. Vandersypen, I.L. Chuang, Rev. Mod. Phys. 76 (2005) 1037.
[26] K.S. Novoselov et al., Science 315 (2007) 1379.
[27] N.A. Besley, J.J. Titman, M.D. Wright, J. Am. Chem. Soc. 127 (2005) 17948.
[28] L.J. Schulman, U. Vazirani, in: Proceedings of the 31st Annual ACM Symposium on Theory of Computing (STOC 99), 1999, p. 322.